CROI 2025

585

HIV Reservoir in Jejunum Exhibit Distinct Phenotypic Features and Evoke Innate Cell Redistribution.

Marta Calvet-Mirabent[1], Monet Yuan[1], Xiaoyu Luo[1], Julie Frouard[1,2], Jason Neidleman[1, 2], Ashley F. George[1], Stan Tamaki[3], Antoine Chaillon[4], Elizabeth Hastie[4], Davey Smith[4], Collin Kieffer[5], Sara Gianella[4], Nadia R. Roan[1, 2]

[1]Gladstone Institute of Virology, University of California San Francisco, San Francisco, CA, USA; [2] Department of Urology, University of California San Francisco, San Francisco, CA, USA; [3] Parnassus Flow Cytometry Core, University of California San Francisco, San Francisco, CA, USA; [4] Department of Medicine, University of California San Diego, La Jolla, CA, USA.; [5] Department of Microbiology, University of Illinois at Urbana-Champaign, Urbana, IL, USA.

BACKGROUND

Gut-associated lymphoid tissue (GALT) is a preferential site for HIV-1 persistence during ART, and previous studies using an SIV infection model suggested that of all the lymphoid tissues, the GALT might represent the largest reservoir. Little is known about the phenotype of the HIV-1 reservoir cells or the influence of the local microenvironment in the different GI regions. In this study, we used standard and 40-parameter multiplexed ion beam imaging by time of flight (MIBI-TOF) microscopy to study the HIV reservoir and their associated environments from 5 different regions of the gut of ART- suppressed PWH (ART-PWH).

METHODS

Fresh tissue specimens from duodenum (DDM), jejunum (JJM), ileum (ILM), colon (CLR) and rectum (RCT) were obtained through the Last Gift rapid autopsy program from n=6 ART-PWH and n=2 people without HIV (PWOH).
Briefly, tissues were fixed and paraffin-embedded (FFPE) and prepared for multiplexed RNAscope (to detect HIV RNA) and confocal immunofluorescence imaging (to detect HIV p24 and CD4). A subset of the samples was used for MIBI-TOF imaging following standardized protocols (**Figure 1**). The stained slides were imaged with an Ionpath MIBIscope targeting areas with increased infiltration of immune cells defined by Hematoxylin & Eosin staining. Images were analyzed using ImageJ2 v2.14.0, R v4.3.2 and GraphPad Prism v10.1.0 software.

Figure 1

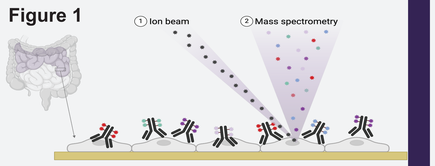


Figure 1. Schematic of MIBI-TOF experimental procidure representing tissue staining and imaging.

RESULTS

Firstly, we assessed the presence of active reservoir cells in 5 different anatomical areas of the gut of n=6 suppressed PHW. We combined the detection of HIV-1 RNA using *in situ* hybridization with probes targeting the gag-pol region, and the detection of HIV-1 protein by targeting p24 alongside with CD4 staining. While on average 85% [74-100%] of the HIV RNA+CD4+T cells in the DDM, CLR, and RCT expressed p24, only 45% [25-79%] in the JJM and ILM were p24+ (**Figure 2**).

Figure 2

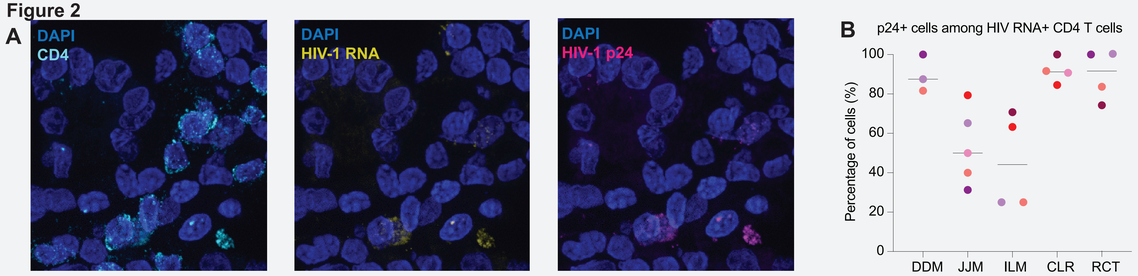


Figure 2. *Identification of HIV-1 RNA+ and protein+ cells in the mucosa and submucosa of the different areas of the gut of suppressed PWH.* **A**: Image and magnification of a section of the mucosa of an ART-suppressed PWH showing nuclear staining (DAPI, dark blue), HIV-1 p24 detection (cyan) and HIV-1 RNA detection (red). Overlay of the three channels is shown on the left, and single channels for HIV-1 p24 detection and HIV-1 RNA detection are shown on the right. **B**: Quantification of HIV-1 p24+ cells among the HIV-1 RNA positive CD4+ T cells in the different gut compartments, each color representing one of the n=6 ART suppressed PWH. Missing dots stand for missing tissue or inexistence of CD4 T cell infiltration in the tissue.

To test the hypothesis that immune-mediated recognition and depletion of p24+ cells may be occurring in the JJM and ILM, we used MIBI-TOF to assess phenotypic features of the p24+ cells and their local environment in JJM of an ART-PWH. Among the 354 CD4 T cells that we identifiedin the jejunum section, 6 had high expression of HIV-1 p24 in the ART-suppressed PWH; these were all exclusively among CD4 T cells from the PWH (**Figure 3 A-B**). Relative to uninfected CD4+ T cells, p24+CD4+ T cells expressed higher levels of HIV coreceptor CCR5, different checkpoint receptors (PDL1 and TIGIT), Tfh marker CXCR5, inflammatory and cytotoxic markers (Galectin-9 and Granzyme B), proliferation marker Ki67, and differentiation marker AIOLOS compared to the HIV-1 negative CD4 T cells from the same region (**Figure 3 C**).

We evaluated the different immune cells composing the local environment in JJM of an ART-PWH, and we analyzed the distance of the different cells to the closest HIV p24+ CD4+ T cell. These p24+ cells were in closer proximity to NK cells and dendritic cells (DCs) than to other subsets including B cells, CD8+T cells, monocytes and macrophages (**Figure 4 A-B**). When analyzing the total number of cells per population, the overall numbers of macrophages were significantly decreased in the JJM of ART-PWH compared to the JJM of PWOH (**Figure 4 C**).

RESULTS

Figure 3

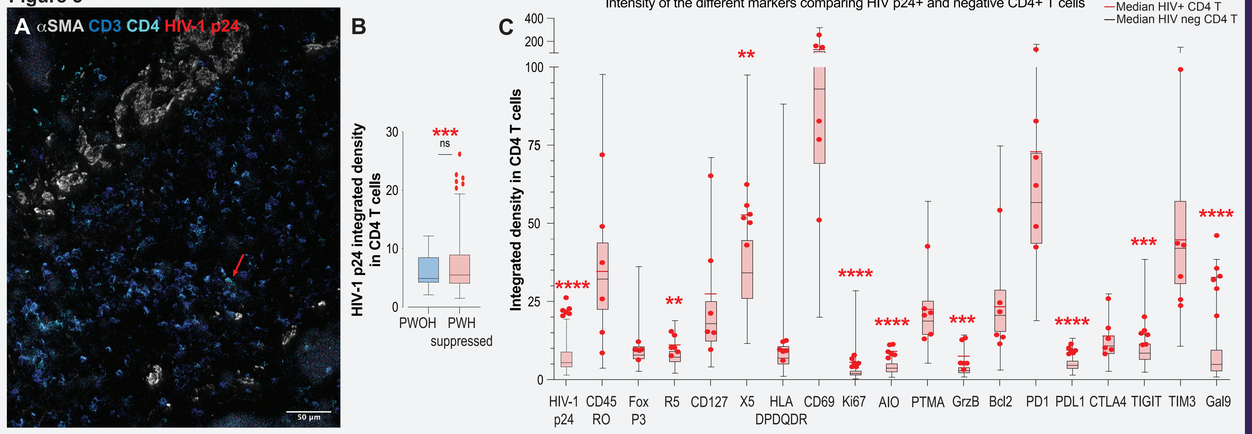


Figure 3. *Phenotypical differences of HIV-1-infected and non-infected CD4 T cells in the mucosa and submucosa of the jejunum of a suppressed PWH.* **A**: Image of a section of the mucosa of an ART-suppressed PWH showing the endothelial marker αSMA (light gray), the T cell markers CD3 (dark blue) and CD4 (cyan), and HIV-1 p24 (red). The red arrow highlights the HIV-1 p24 CD4 T cell. **B**: Quantification of HIV-1 p24 integrated density in CD4 T cells. Red dots highlight the 6 HIV-1 p24+ CD4 T cells. Statistical significance was calculated using two-tailed Mann-Whitney U test comparing CD4 T cells from PWOH *vs* HIV-1-negative CD4 T cells (black) or the HIV-1 p24+ CD4 T cells (red; ***p<0.001) from the PWH. **C**: Quantification of integrated density for each of the markers described. Box and whiskers represent the values for the 348 HIV-1 negative CD4 T cells detected in the ART-suppressed PWH, while the red dots highlight the 6 HIV-1 p24+ CD4 T cells detected in these same regions. Statistical significance was calculated using two-tailed Mann-Whitney U test comparing HIV-1-negative *vs* HIV-1 p24+ CD4 T cells from the same ART-suppressed PWH (**p<0.01, ***p<0.001, ****p<0.0001). R5 = CCR5, X5 = CXCR5, AIO = AIOLOS, GrzB = Granzyme B, Gal9 = Galectin-9.

Figure 4

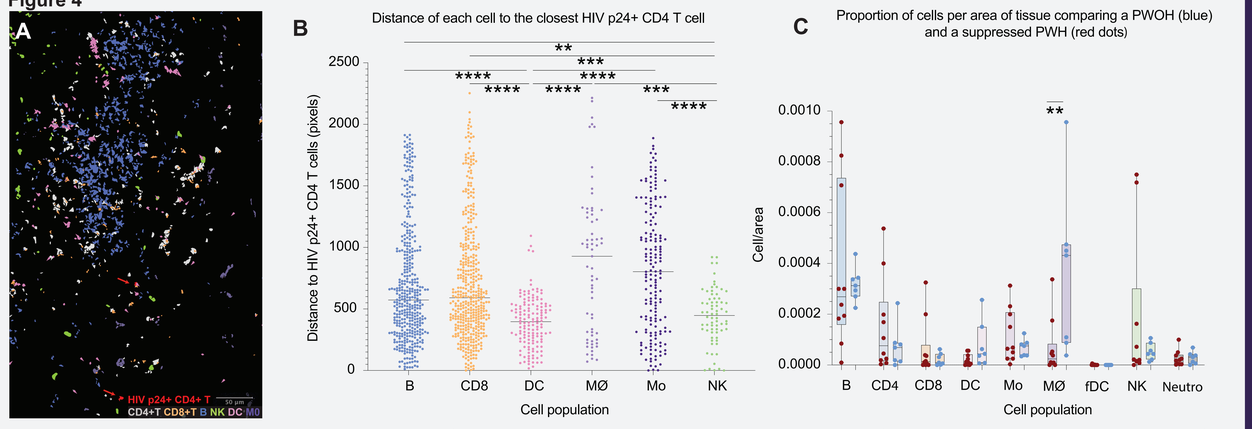


Figure 4. *NK cells and dendritic cells are closer to the HIV p24+ CD4+ t cells than other immune cell populations in the jejunum of an ART suppressed PWH.* A: Representation of the identification of the different cell populations in the same image shown in Figure 3A. The images highlights CD4+ T cells (light gray), CD8+ T cells (orange), B cells (blue), NK cells (green) and macrophages (purple, MØ). In read and highlighted with a red arrow we show the HIV p24+ CD4+ T cells. B: Quantification of the distance of each cell to the closest HIV p24+ CD4+ T cell. Statistical comparison between immune populations was calculated using one way ANOVA Kruskal-Wallis multiple comparison test (**p<0.01, ***p<0.001, ****p<0.0001). C: Respresentation of the quantification of number of cells per area of each image comparing the mucosa and submucosa areas of an ART-suppressed PWH (maroon) and a PWOH (blue). Statistical significance was calculated using two-tailed Mann-Whitney U test (**p<0.01).

CONCLUSIONS

Our data suggest that HIV p24+ CD4+T cells are distributed throughout the entire gut of ART-PWH, but that **JJM and ILM may possess distinct mechanisms that preferentially eliminate these cells. p24+ cells in JJM of ART-PWH exhibit distinct phenotypic features including evidence of recent proliferation (Ki67)**. Their spatial localization suggests **recruitment of subsets of innate cells (NK cells and DCs)**, which can help eliminate infected cells.

Overall, our results point to active crosstalk between HIV-infected cells and innate immune effector cells in the gut of ART-PWH.

GLADSTONE INSTITUTES UCSF Last Gift UCSF-BAY AREA CFAR CENTER FOR AIDS RESEARCH HIV CARE Collaboratory of AIDS Researchers for Eradication HOPE HIV Obstruction by Programmed Epigenetics